J Mater Sci (2007) 42:8599–8605
DOI 10.1007/s10853-007-1861-x

Study on synthesis and properties of hydroxyapatite nanorods and its complex containing biopolymer

Fangzhi Huang · Yuhua Shen · Anjian Xie · Jinmiao Zhu · Chunyan Zhang · Shikuo Li · Jun Zhu

Received: 18 December 2006 / Accepted: 18 May 2007 / Published online: 10 July 2007

Abstract Regular hydroxyapatite nanorods were synthesized using polyethylene glycol as chemical additive and determined by Fourier transform infrared spectrometer, X-ray diffraction and transmission electron microscope. The results showed that irregular quadrate polyethylene glycol/hydroxyapatite complex had formed in the aqueous solution, then hydroxyapatite nanorods with the diameter of about 10–15 nm and the length of 30–50 nm were obtained after calcining. The optimum calcining temperature was 500 °C. Nucleation and growth mechanism of the hydroxyapatite nanorods was illustrated. In addition, the stability of the HAP nanorod in the aqueous suspended solution was also considered. The addition of dispersant such as sodium chloride, kalium chloride and sodium dodecyl sulfonate was helpful for the stability of suspended hydroxyapatite nanorod and the mechanism was discussed. Dextran/hydroxyapatite complex with homogeneous size distribution was synthesized, and significant improvements in the mechanical properties were obtained for sintered specimens of the dextran/hydroxyapatite complex in comparison to pure HAP.

F. Huang · Y. Shen (✉) · A. Xie · J. Zhu · C. Zhang · S. Li · J. Zhu
School of Chemistry and Chemical Engineering, Anhui University, Hefei 230039, China
e-mail: s_yuhua@163.com

Y. Shen · A. Xie
State Key Laboratory of Coordination Chemistry, Nanjing University, Nanjing 210093, China

Introduction

Hydroxyapatite (HAP) with the chemical formula $Ca_{10}(PO_4)_6(OH)_2$ is one of the most biocompatible materials owing to its similarity with mineral constituents found in hard tissues (such as teeth and bones) [1–4]. Especially, it can be used in medical field for implant fabrication [5]. Some of these applications require highly densified ceramic materials, which exhibit a high enough mechanical strength for loadbearing. Hydroxyapatite ceramics have excellent fatigue resistance if properly made without pores or second phases [6]. HAP biomaterials physical properties such as fracture toughness and fracture strength, etc. can be tailored over wide range by control of particle size and the crystal structure [7]. In this case, preparing a fine and sinterable hydroxyapatite such as hydroxyapatite nanorods is the first and perhaps the most important step in achieving this goal because HAP phase present in natural bone is nanorod with the diameter of 20 nm and a length of 40–60 nm. So far, a lot of works have been done in order to obtain nano-sized and weakly agglomerated HAP powder, such as hydrothermal treatment [8], microemulsion/inverse microemulsion route [9], precipitation process [10] and wet chemical technique [11]. Nano-sized HAP rods, which are similar to natural HAP nanorods in diameters and lengths and properties, have not been produced, whereas some of these methods can produce high quality powders. So the synthesis of HAP nanorods with suitable size is still of urgency and significance.

In our work, regular HAP nanorods were synthesized using PEG 300 as chemical additive, which is a non-toxic, biodegradable, non-ionic surfactant. The diameter and length of the nanorods were very similar to those of HAP rods of natural bone. The nucleation and growth mechanism of the HAP nanorods was put forward, and the

stabilities of the suspended nanorods influenced by different dispersant such as electrolyte and surfactant were also discussed in detail. The HAP nanorods and crude dextran were easy to combine to form new dextran/HAP complex by simple ultrasonication. It can be used widely in medical field, because dextran (Scheme 1) is a non-reducing, biologically inert amylase and abundant in living organism, and helpful to reinforce its biocompatibility.

Experiments

Chemicals

Polyethylene glycol (M.W. 300), dextran (M.W. 9,000) and poly (ε-caprolactone) (PCL, M.W. 80,000) were obtained from Aldrich Chemical Co. and used without further purification. Calcium chloride ($CaCl_2$), sodium hydrogen phosphate (Na_2HPO_4), sodium chloride (NaCl), kalium chloride (KCl), sodium dodecyl sulfonate ($CH_3(CH_2)_{11}SO_3Na$) were all analytical purity.

Instruments and characterizations

The samples of hydroxyapatite complex (in proportion of 1% in KBr powder) were performed and recorded with a Fourier transform infrared spectrometer Niolet 870 between 4,000 cm^{-1} and 400 cm^{-1} with a resolution of 4 cm^{-1}. The XRD measurements were performed by a X-ray diffractometer (rigakvD/Max RA) at a scanning rate of 4°/min, using a monochromatized Cu Kα radiation (λ = 0.154 nm). The morphologies were routinely observed by TEOLTEM-100sx transmission electron microscopy. The particle size distribution as determined using photon correlation spectroscopy was measured by a Zetasize 3000HSA apparatus (from Malvern Instruments, UK), with the same instrument we can also measure the Zeta potential of the particles.

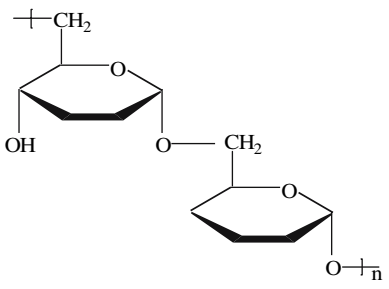

Scheme 1 Molecular structures of dextran

Preparations of samples

A 50 mL 0.05 mol/L $CaCl_2$ aqueous solution was prepared by adding appropriate PEG (1.5 wt%) as chemical additive and kept overnight (about 12 h) to ensure the cooperative interaction and self-assembly process completion. The above solution was added dropwise into 50 mL 0.03 mol/L Na_2HPO_4 aqueous solution with constant mechanical stirring (stirring rate, 1,000 rpm). The resultant solution was aged up to 48 h in a sealed glass vial and centrifugated at 15,000 rpm to obtain the solid product.

The solid product was washed three times with double-distilled water, absolute ethyl alcohol, respectively, and dried at 60 °C on a stainless crucible, giving rise to the formation of as-prepared powder. The as-prepared powder was divided into five parts, and calcined at 300 °C, 500 °C, 700 °C, 900 °C, 1,100 °C for 2 h, respectively. Then, hydroxyapatite particles were obtained.

The as-prepared powder and hydroxyapatite particles were dispersed by ultrasonic dispersion in deionized double-distilled water. The particle sizes distribution or morphologies were observed. Finally, hydroxyapatite particle obtained by being calcined at 500 °C was dispersed in NaCl, KCl and sodium dodecyl sulfonate aqueous solution, respectively.

Sedimentation tests were performed as follows. The dispersions in aqueous solutions were prepared by adding amount of hydroxyapatite powders in the deionized double-distilled water with various dispersants and then the mixtures were ultrasonicated for 10 min. The concentration of all dispersions was 0.5 vol%. After ultrasonication, the dispersions were poured into a clear 10 mL graduated test tube. The change of flocculated sediment height with time was recorded from 3 h to a week.

Preparation and characterization of biopolymer/HAP complex

Experiment was performed by equilibrating 0.25 g of HAP nanorod with 50 mL of dextran aqueous solution with the concentration of 0.5 wt%. The suspension was ultrasonicated for 24 h in order to ensure the adsorption equilibrium. The solid of HAP preadsorbed with polymer was obtained after centrifugated, washed and dried.

Five milligrams of HAP preadsorbed with dextran were suspended in 50 mL deionized double-distilled water. After equilibration the electrophoretic mobility and the morphology of the complexes were observed.

All the experiments were carried out at room temperature (25 °C), and pH of the solutions was adjusted to 8.6 with diluted NaOH or HCl aqueous solutions during the experiment process.

Mechanical testing [12]

HAP and dextran/HAP were dispersed separately in methylene chloride, and PCL was added to each suspension to make the solution mixture. Each solution was poured into an excess of *n*-hexane to precipitate the HAP/PCL and dextran/HAP/PCL nanocomposites, respectively. The composites were dried in vacuo at room temperature for 24 h. For preparing specimens for tensile testing, pure PCL and the nanocomposites of HAP (10 wt%)/PCL, (dextran/HAP) (10 wt%)/PCL were compressed by hot press molding at 100 °C and 15 MPa. The sample specimens with the dimension of 35- 5–0.5 mm^3 were cut. The tensile test was performed using a computer controlled mechanical Universal testing machine LLOYD LR50 K (Fareham, UK) at a stretching rate of 20 mm/min and cross-head speed of 20 mm/min.

Results and discussion

Influence of calcining temperature on HAP particle size

Particle size and distribution of HAPs calcined at different temperatures was shown in Fig. 1. When as-prepared HAP was calcined at 300 °C, 500 °C, 700 °C, 900 °C, 1,000 °C the obtained HAP particle size was 80 nm, 35 nm, 56 nm, 90 nm, 110 nm, respectively, and the peak of size distribution was the sharpest when calcining temperature was 500 °C. It indicated that 500 °C was the optimum calcining temperature to obtain the HAP nanoparticles with the smallest particle size and the best size distribution.

Characterization of HAP nanoparticles

The TEM micrographs (Fig. 2) shows morphologies of as-prepared HAP and HAP obtained by being calcined at 500 °C. The as-prepared HAP was irregular quadrate particle (shown in Fig. 2a) with the dimension of 40 × 60~120 nm. When it was calcined at 500 °C, the morphology changed and inerratic nanorods appeared (shown in Fig. 2b). The diameter of the nanorod was about 10–15 nm and the length was about 30–50 nm.

Figure 3 illustrates the FT-IR spectra of the as-prepared HAP and HAP nanorods. It shows strong $-PO_4^{3-}$ stretching modes occurring at 1,035 cm^{-1} and bending stretching modes at 569, 605 cm^{-1}. Absorbed water bands located at 1,600–1,635 cm^{-1} and 3,000–3,700 cm^{-1} overlapped the –OH interference at 3,572 cm^{-1}. The peaks at 2,924, 1,385 cm^{-1} and 1,103 cm^{-1}, typical for –CH and C–O–C stretching, respectively, reflected the presence of polyethylene glycol, and were clearly observed in FT-IR spectrum of the as-prepared HAP (Fig. 3a), but they were too weak to be observed in that of the HAP nanorods (Fig. 3b). The results indicted that the nanorods were only composed of HAP.

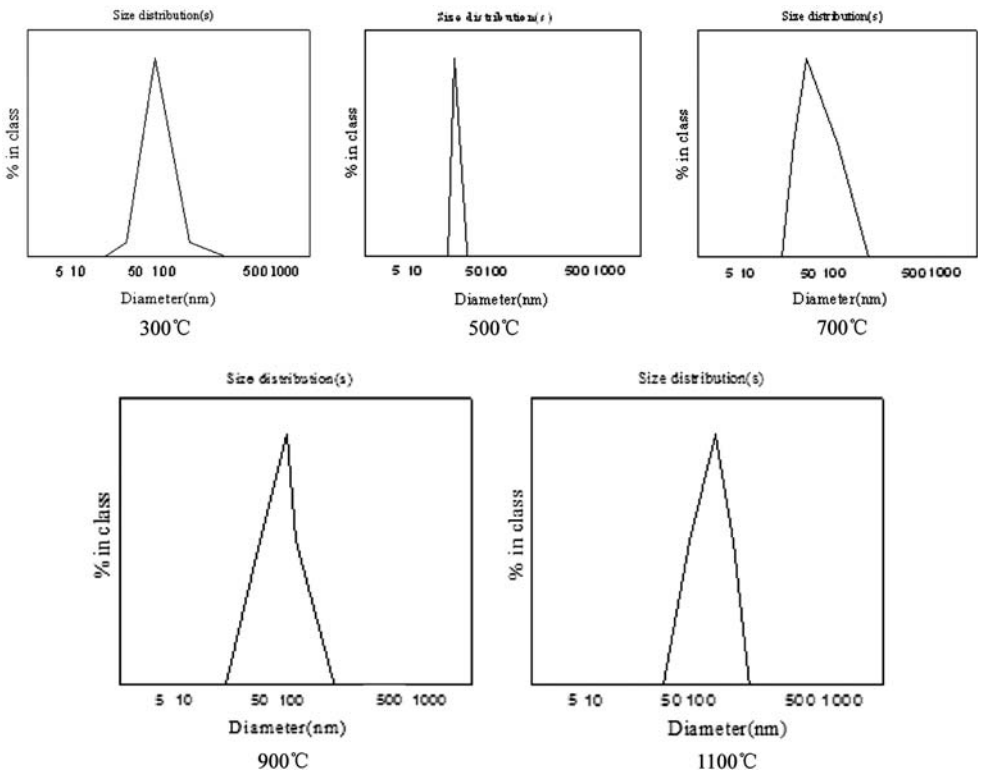

Fig. 1 Particle size and distribution of HAPs calcined at different temperatures

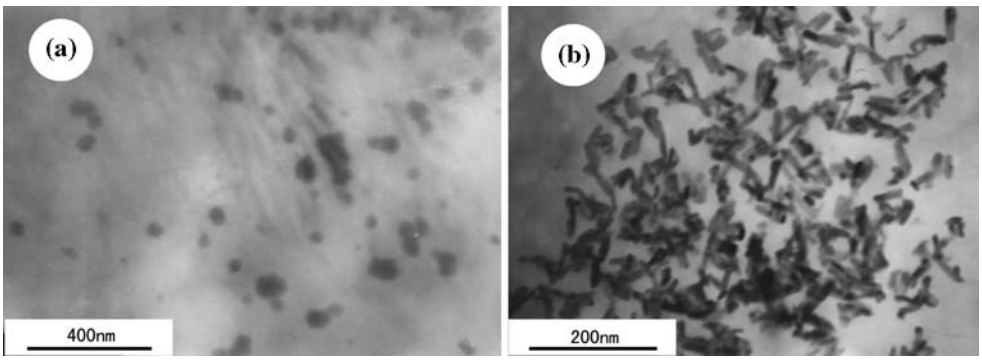

Fig. 2 TEM of the as-prepared HAP (**a**) and HAP nanorods (**b**)

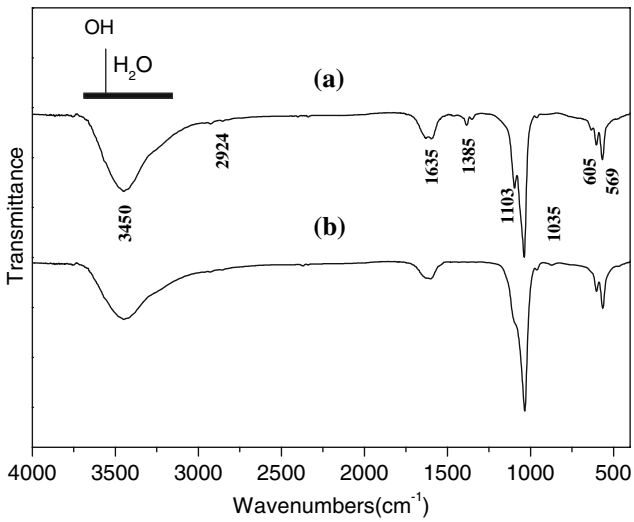

Fig. 3 FT-IR spectra of the as-prepared HAP (**a**) and HAP (**b**) calcined at 500 °C

The XRD pattern given in Fig. 4 shows the characteristic diffraction reflection of HAP nanorods. The characteristic peaks at 2θ regions of 26°, 29°, 32–34°, 40°, and 46–54° indicated the crystalline nature of HAP nanocrystals [12]. As shown in Fig. 4, the reaction did not induce any change in crystallinephase of HAP nanocrystals and the reflection planes matched with the JCPDS files of HAP crystal. The wide and high peaks revealed that the HAP nanorods had a small size and good crystal quality.

Zeta potentials of HAP nanorods in suspensions with different dispersants

Figure 5 shows the zeta potential curves of the HAP nanorods plotted as function of concentration of electrolytes (NaCl or KCl). The zeta potentials of HAP nanorods were about –13.4 mV in the absence of electrolytes, and the suspended HAP nanorods had a tendency to aggregate in the suspension (shown in Fig. 2b). After the addition of NaCl, we observed an initial increase in the absolute value of the measured zeta potential with respect to the samples without adding NaCl, and it was up to a maximum (17.3 mV) when the concentration of NaCl reached was 0.01 mol/L. When NaCl concentration exceeded the critical value, the absolute value of zeta potential would

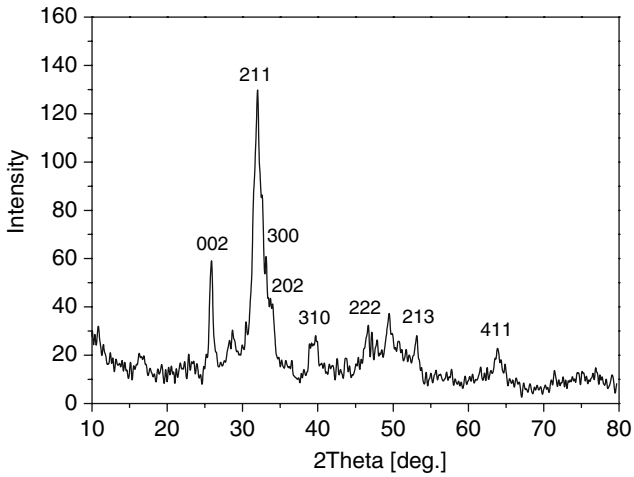

Fig. 4 XRD pattern of HAP nanorods obtained at the calcining temperature of 500 °C

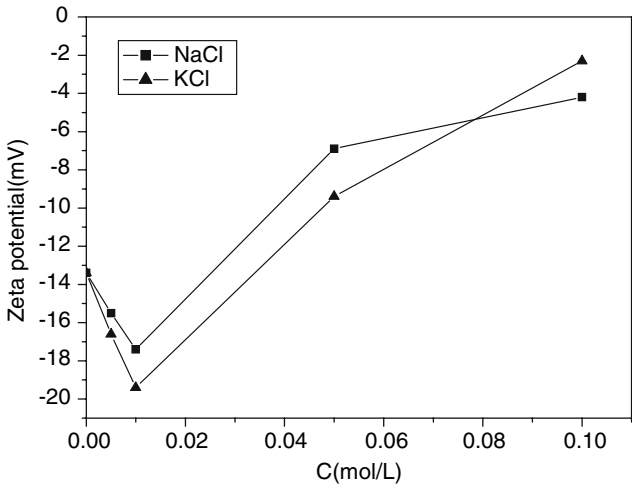

Fig. 5 Zeta potential of HAP nanorods in the presence of dispersants

decrease with the increase of the NaCl concentration. Using KCl as dispersant, it showed the same influence on the zeta potential of suspended HAP nanorods except that the maximal absolute value of the zeta potential could reach 21.0 mV. The variety of the zeta potential might be due to the formation and change of HAP nanorod electric double layer. According to the Gouy–Chap–Stern theory, the solution conductivity would increase when an appropriate quantity of electrolytes were added, which would accelerate the formation of suspended HAP nanorod electric double layer and result in the increase of zeta potential in magnitude. But, the electrolyte in high enough concentration compressed the structure of electric double layer, which led to decrease the absolute value of zeta potential. The electric repulsive force amongst the suspended HAP nanorods would increase when the absolute value of zeta potential increased, which was helpful for the stability of HAP nanorods in suspended solution. That is to say, the stability of suspended HAP nanorods could be enhanced by the addition of electrolytes with certain concentration. If the electrolyte was NaCl or KCl, the optimum concentration was 0.01 mol/L. The morphologies of the well-dispersed HAP nanorods in 0.01 mol/L NaCl solution were shown in Fig. 6a.

When sodium dodecyl sulfonate (SDS) replaced NaCl as dispersant, the zeta potential of the suspended HAP nanorods increased to 38.0 mV in the magnitude, and there was a more homogeneous dispersal of HAP nanorods in the suspended solution (shown in Fig. 6b). In aqueous suspended solution, in spite of the electrostatic repulsion forces existing between the HAP nanorods and SDS (both negatively charged), the zeta potential value increased on the addition of 1 wt% SDS. This result may be due to the presence of a specific interaction such as a chemical interaction (the attractive interaction between surfactant anion and Ca^{2+} on the surface of HAP particle), hydrogen bonding, or a combination of the two mechanisms. At the same time, because the repulsive force amongst the HAP nanorod particles would increase with the increase of zeta potential value, the stability of the suspended HAP nanorod particles would be reinforced. All these indicated that the stabilities of the HAP nanorods in suspended solution could be further enhanced by the addition of SDS dispersant.

Sedimentation tests were conducted to evaluate the stability of dispersions, as sedimentation tests are easily carried out and yield direct information concerning the technological uses of the dispersions [13]. The flocculation rate which can be indicated by the change of the upper level of the flocculated sediment was a good indicator to the stability of dispersions. Figure 7 shows the change of sediment height as function of time in aqueous solutions. Stratification took pace in half an hour after ultrasonication, and the sediment height in these dispersions was near the lowest point after 48 h. In aqueous solutions with dispersants (sodium chloride, sodium dodecyl sulfonate), the settlement rate was slower than that without any dispersant. The best stability of dispersions was found in the sodium dodecyl sulfonate aqueous solutions.

Characterization of dextran/ HAP complex

The TEM micrograph of dextran adsorbed HAP complex was presented in Fig. 8. It revealed the presence not only of numerous irregular particles but also of elliptical particles. The size of particles was approximately 60 nm and 50 nm in major and minor diameter. The zeta potential of the aqueous suspended complex particles reduced to –44.2 mV. The particle size and the value of the zeta potential were seen to increase with the absorption of dextran in suspension. Additionally, according to the FT-IR spectrum of the complex, a small amount of $–CH_2$ was recorded around 2,852 cm^{-1}, 2,926 cm^{-1}. The results showed that dextran and HAP nanorod cores had combined to form a dextran/HAP complex.

The data on the mechanical properties of HAP and dextran/HAP samples are presented in Table 1. It is apparent from Table 1 that the sample containing dextran/ HAP has improved values of tensile modulus, tensile

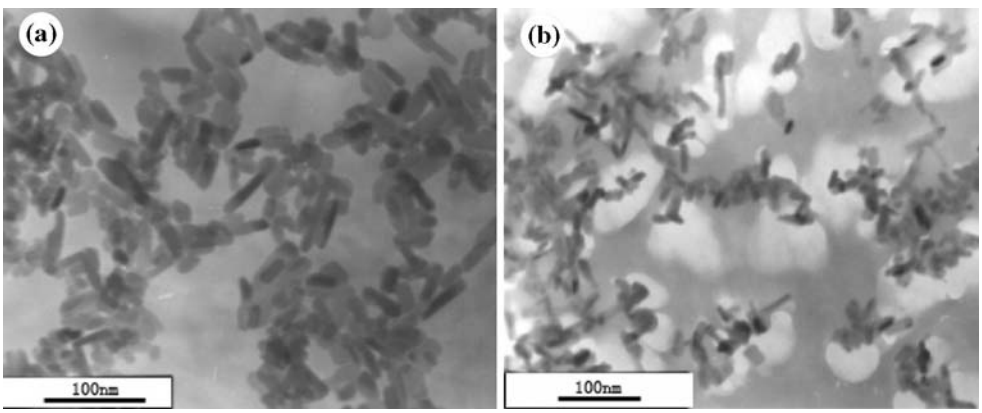

Fig. 6 TEM of HAP nanorods in the suspensions containing NaCl (**a**) and SDS (**b**)

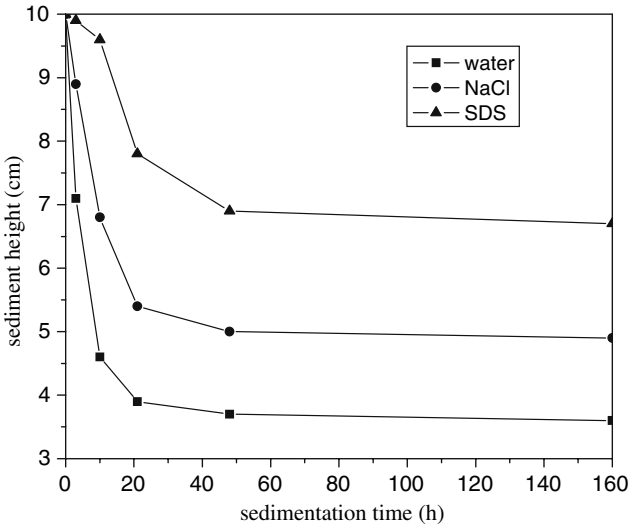

Fig. 7 The change of sediment height as function of time in aqueous solutions

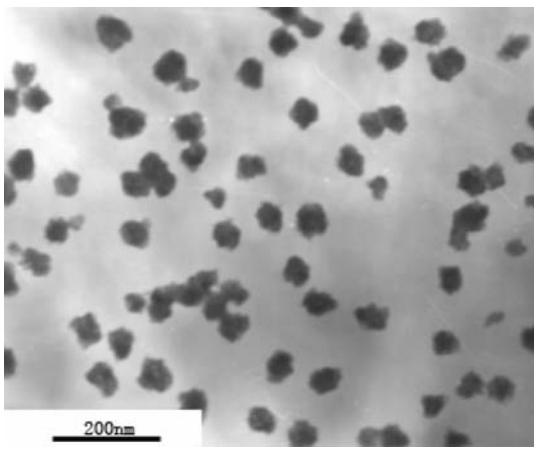

Fig. 8 TEM of dextran/HAP complexes

strength, and ultimate elongation at break in comparison to those of the HAP sample.

Possible nucleation and growth mechanism of HAP nanorods and dextran/HAP complex

In our work, the HAP nanorods were synthesized successfully using PEG as chemical additive and it was probably that PEG could serve as a soft template in the whole experiment process.

PEG is a surfactant with the hydrophilic groups (–O–) and hydrophobic groups ($–CH_2–CH_2–$). The PEG molecule could easily form long chain structure with hydrophilic groups exposed and hydrophobic groups embedded in aqueous solution (shown in Fig. 9). In PEG and $CaCl_2$ mixed solution, the lone-pair of electrons of O atoms of PEG molecules appeared to exert the ability of binding calcium ion, many Ca^{2+} ions would accumulate on the surface of PEG long chain, and the OH^- and PO_4^{3-} ions would also assemble there by electrostatic interaction when Na_2HPO_4 was added into the solution. The increase of the supersaturation degree of hydroxyapatite on the PEG molecular surface would trigger the initial nucleation of hydroxyapatite. The O atoms of PEG long chain would serve as the nucleation site of HAP and induced the heterogeneous nucleation of HAP (shown in Fig. 10a, b). The HAP crystal would also trend to grow and aggregate along the PEG long chains (shown in Fig. 10c, d). Thus, the HAP nanorods formed with the inducing of PEG template as the arrangement of ions–nucleation–growth–aggregation model (A-N-G-A model) described.

Conclusion

In summary, HAP nanorods with an aspect ratio of 3–5 were prepared using PEG as chemical additive. During the experiment, PEG was incorporated into the formation of as-prepared HAP and removed by calcining, and the optimum calcining temperature was 500 °C. An A-N-G-A model may illustrate the formation mechanism of HAP nanorod. Dispersibility and stability of the hydroxyapatite nanorods were also discussed based on the measurement of zeta potential and morphology in the absence or presence of different dispersants. The addition of electrolyte such as sodium chloride and kalium chloride was helpful to prevent the aggregation of hydroxyapatite nanorods in suspension, the stability of suspended hydroxyapatite nanorods would be further enhanced by the addition of sodium dodecyl sulfonate. Dextran/HAP complex with homogeneous size distribution was synthesized successfully and its mechanic properties were enhanced compared to pure HAP.

Table 1 Mechanical Properties of PCL, HAP/PCL and dextran/HAP/PCL

Sample	Tensile modulus (MPa)	Tensile strength (MPa)	Ultimate longation at bteak (%)
Pure PCL	2.6	20.5	214.6
HAP (10 wt%)/PCL	3.4	22.6	141.2
(Dextran/HAP) (10 wt%)/PCL	6.1	29.8	278.4

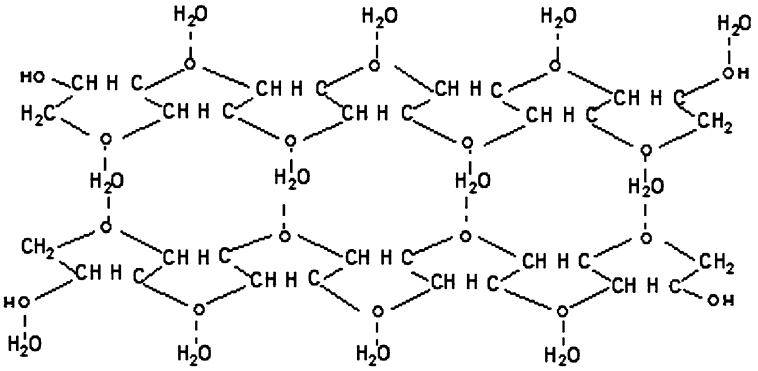

Fig. 9 The structure of PEG molecule in water solution

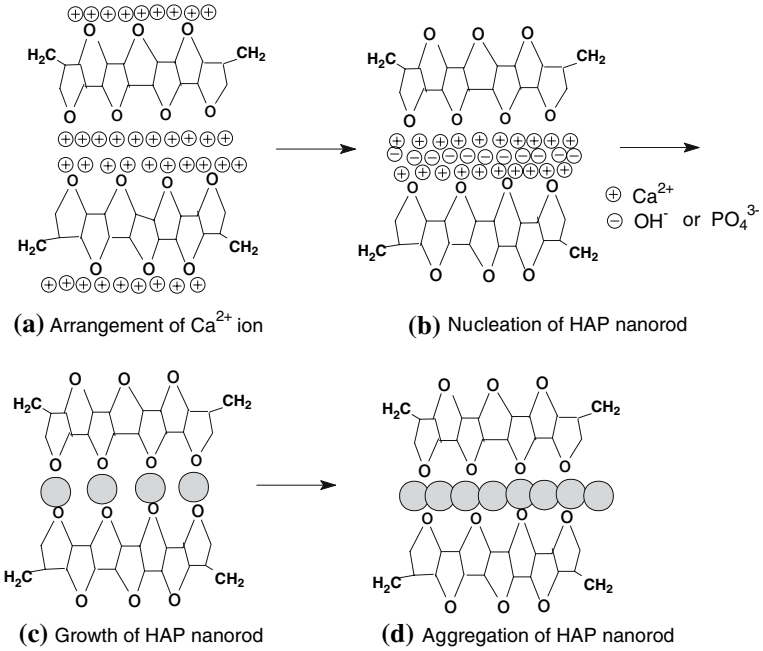

Fig. 10 Possible mechanism of HAP nanorod nucleation and growth

Acknowledgements This work is supported by the National Science Foundation of China (20471001 and 20371001), and the Specific Project for Talents of Science and Technology of Universities of Anhui Province (2005hbz03).

References

1. Verestiuc L, Morosanu C, Bercu M, Pasuk I, Mihailescu IN (2004) J Cryst Growth 264:483
2. Kaneko T, Ogomi D, Mitsugi R, Serizawa T, Akashi M (2004) Chem Mater 16:5596
3. Suchanek WL, Shuk P, Byrappa K, Riman RE, Huisen KST, Janas VF (2002) Biomaterials 23:699
4. Lin FH, Liao CJ, Chen KS, Sun JS (2000) Mat Sci Eng C 13:97
5. Cheng K, Shen G, Weng WJ, Han GR, Ferreira JMF, Yang J (2001) Mater Lett 51:37
6. Bose S, Saha SK (2003) Chem Mater 15(23):4464
7. Riman RE, Suchanek WL, Byrappa K, Chen CW, Shuk P, Oakes CS (2002) Solid State Ionics 151:393
8. Li Y et al (1994) J Mater Sci: Mater Med 5:326
9. Lim GK et al (1999) Langmuir 15:7472
10. Xiao F, Ye JD, Wang YJ, Rao PG (2005) J Mater Sci 40:5439 DOI: 10.1007/s10853-005-1919-6
11. Liu YK, Hou DD, Wang GH (2004) Mater Chem Phy 86:69
12. Hong JL, Hyung WC, Kyung JK, Sang CL (2006) Chem Mater 18:5111
13. Chen YZ, Liang Y, Zheng F, Zhou RC, Feng ZC (2001) Ceram Int 27:73